Physics design of CYCAIE-100*

ZHANG Tian-Jue(张天爵)[1)] LI Zhen-Guo(李振国)[1] ZHONG Jun-Qing(钟俊晴)[1]
AN Shi-Zhong(安世忠)[1] YAO Hong-Juan(姚红娟)[1] JI Bin(纪彬)[1] WEI Su-Min(魏素敏)[1]
GUAN Feng-Ping(管峰平)[1] YANG Jian-Jun(杨建俊)[1,2] BI Yuan-Jie(毕远杰)[1,2]
JIA Xian-Lu(贾先禄)[1] WANG Chuan(王川)[1]

1 (China Institute of Atomic Energy, Beijing 102413, China)
2 (Tsinghua University, Beijing 100084, China)

Abstract The design and construction of Beijing Radioactive Ion-beam Facility (BRIF) was started at China Institute of Atomic Energy -CIAE) in 2004. In this project, a 100 MeV high intensity cyclotron, CYCIAE-100, is selected as a driving accelerator for radioactive ion beam production. It will provide a proton beam of 75—100 MeV with an intensity of 200—500 μA. The scheme adopted in this design, i.e., stripping the accelerated H^-, makes the structure more compact and construction cost much lower. At present, the design for each system has been accomplished. This paper depicts the basic physics design of the machine, including its major structure and parameters, beam dynamics and each relevant system, e.g. basic structure of the main magnet, numerical simulation of the RF resonant cavity, axial injection system, central region, and study on crucial physics problems concerning the extraction and beam lines. The major problems encountered during the design of CYCIAE-100 are also summarized in this paper.

Key words cyclotron, main magnet, RF cavity, axial injection, extraction, imperfection field

PACS 29.20.dg, 29.27.-a

1 Introduction

As a driving accelerator for BRIF[1], CYCIAE-100 adopts a compact structure with 4 straight sectors. The H- ions produced by the multi-cusp ion source are accelerated, and the high intensity proton beams are extracted through dual stripping. The extracted beam is 200 μA featured with an energy of 75—100 MeV, which is continuously adjustable. This machine is composed of several systems, including main magnet and coils, RF system, and axial injection lines, extraction and beam lines, etc. In this paper, the basic physics design of machine and its components will be depicted.

2 General designs of CYCIAE-100 and basic beam dynamics

The adoption of a compact structure for CYCIAE-100 can provide strong vertical focusing to meet the requirement of intensive beam acceleration. The carbon foils are used to strip the H^- with very small beam loss during the extraction, the efficiency of which can reach 99% from our calculation and test. In order to reduce the beam loss induced by the Lorentz stripping, the hill field at the outer region is less than 1.4 T. The vacuum dissociation is the other reason inducing beam loss in this H^- machine, which requires the vacuum in the tank better than 5×10^{-6} Pa level on average. For the RF system, it adopts double Dee structure, and the fourth harmonics w.r.t. revolving period of accelerated particles. The resonant cavity of half wave length is completely installed and fixed in the valley of the magnet. Fig. 1 shows the overall structure of CYCIAE-100.

During the acceleration, as is well known, the beam corresponding to different energy has fixed equilibrium orbit. The betatron oscillations around equilibrium orbits at different energies up to 100 MeV are investigated in detail with many magnet struc-

Received 6 January 2009
* Supported by NSFC (10125518)
1) E-mail: tjzhang@ciae.ac.cn

tures and their fields. Figs. 2 and 3 show the static stable area at E=0.1 MeV and the tune diagram in CYCIAE-100 respectively. It is easy to notice that the vertical oscillation frequency is higher than 0.5 at most of the acceleration region and towards 0.7. This is of advantage to upgrade the beam intensity later on.

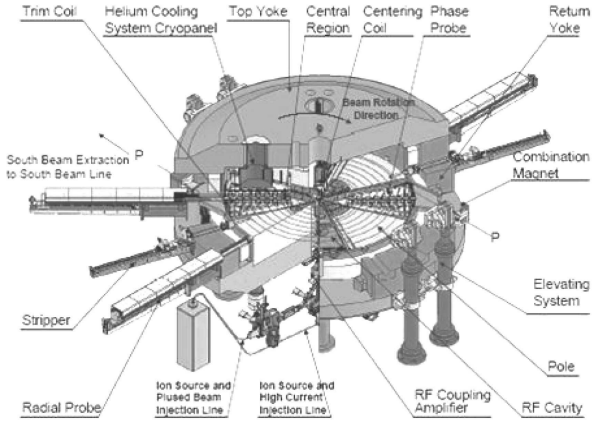

Fig. 1. Lower part of the main magnet.

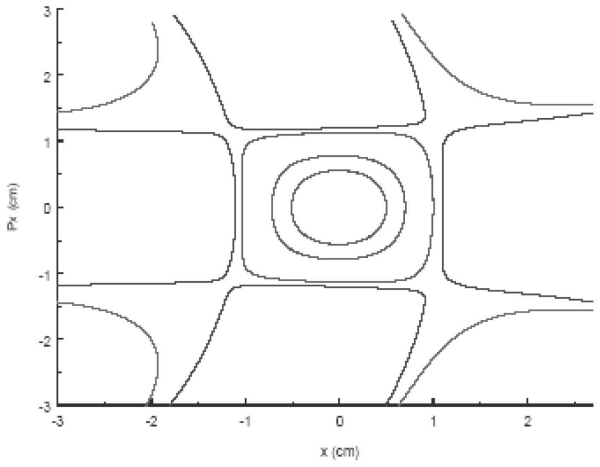

Fig. 2. Radial static region at E = 0.1 MeV.

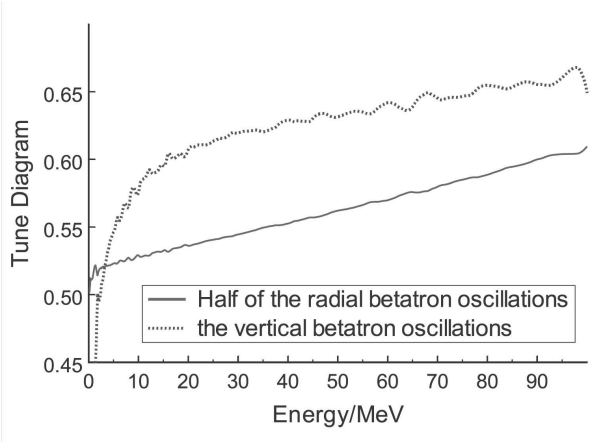

Fig. 3. The vertical and radial betatron oscillation vs energy.

After the static study, the accelerating beam dynamics is also done in detail. The transverse ellipses along the AEO are matched step by step from the central region to final energy. The vertical beam profiles with different RF phases are simulated and multiparticle tracking is carried out to control the beam loss in this small hill gap machine. In practice, the imperfection magnetic field exists and the deviation of the orbit center takes place. Under the influence of the 1st and 2nd harmonic, the beam will oscillate about the deviated orbit center and thus results in its radial dimension growth. In order to obtain a good beam quality, the simulation results show that the magnetic field of the cyclotron should satisfy the following condition: the 1st harmonic is less than 2 Gausses, the 2nd harmonic is less than 40 Gausses, and the gradient of the 2nd harmonic is less than 8 Gausses/cm. To comply with the requirement for being isochronous, it is demanded that the deviation between the measured field at medial plane and the idea field be approximately below 1.05×10^{-4}.

3 Main magnet design

3.1 The structure parameters

In the design of CYCIAE-100, based on the consideration that the beam intensity is increased through the enhancement of vertical focusing and the power consumption of the main coils is reduced by taking a compact structure, the hill gap between the sectors should be small enough. However, taking into account the installation of dummy Dee in the RF system, centering coils, and devices for the beam diagnostics, the hill gap should be sufficiently large. After comparing several solutions, a relatively comprehensive option[2] is adopted, i.e., 6 cm at the central region and gradually changing to 5 cm at the large radius.

In the design, it is required that the isochronous field should be satisfied, and the oscillating frequency in both radial and vertical directions should be under control. Requirements are also set on the negative gradient of the magnetic field and beam centering at the central region. The vertical tune should be large enough at high energy to avoid Walkinshaw resonance and the field distribution in the hill region should be well controlled to make sure that the beam loss induced by Lorentz stripping is less than 0.3%. After adjusting the dimension of each part for the main magnet, e.g. the pole angle, shape of central plug, hill and valley gap, offset of the pole from the machine center, etc., the result from numerical sim-

ulation shows that the magnetic field at the medial plane roughly meets the isochronous, and the integral phase shift is within ±10°. The vertical tune ν_z increases along with the radius and successfully avoids all the harmful resonances at high energy.

To limit the magnet deformation, the shape of the top/bottom yoke is optimized. The FEM simulation is performed for even height and many uneven height structures of top/bottom yoke. The results show that when the weight of the main magnet remains unchanged and one of the optimized solutions of uneven height top/bottom yoke is able to reduce the deformation by 40% compared with the solution of even height. Table 1 indicates the structural parameters of the main magnet for CYCIAE-100.

Table 1. Main parameters of magnet (unit: mm).

radius of poles	2000	height of magnet	2820
angle of poles	47°	inner diameter of coils	4192
gap	50—60	outer diameter of coils	4734
height of coils	362	inner diameter of yoke	4820
ampere-turn	29800	outer diameter of yoke	6180

3.2 Imperfection field

To get a precise prediction of the distribution of imperfection field brought about from the non-uniformity of the magnet material and the imperfection factors during the heat treatment, and to effectively reduce the design and construction risks of the key part as the main magnet, those potential problems are simulated and studied through FEM analysis.

At the stage of casting and forging, gas bubbles and impurity often appear inside the steel. These defects will give impact to the magnetic field distribution. Therefore various simulations are carried out to clarify the influence to the magnetic field at different locations by defects of different size. Fig. 4 shows the permitted defect in three zones of the magnet, and the detail is shown in Table 2.

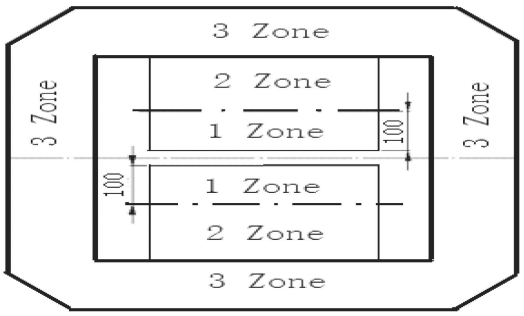

Fig. 4. Three zones for ultra-sonic detection.

Table 2. Tolerant defect of each zone in the magnet.

division	equivalent diameter	in an area of 200 mm×200 mm, less than 5 equivalent diameter
1 Zone	Φ3 mm	Φ2 mm
2 Zone	Φ6 mm	Φ4 mm
3 Zone	Φ8 mm	Φ6 mm

To determine the relation between the difference of BH curves of the steel for sectors and the 1st harmonic at the medial plane, the BH curve of 1008# Steel is taken as reference. The magnetic permeability for one of the four pairs of sectors is reduced by 1%, and the other three pairs remain unchanged. The numerical simulation result shows that the amplitude of the 1st harmonic increases along with the radius, but the largest amplitude for the 1st harmonic is no more than 8 Gausses. According to the basic result from numerical simulation, the deviation for the magnetic permeability between sectors should be within 1.5%, which can be compensated during the mapping and shimming of the magnet.

While the top/bottom yoke is under casting and heat treatment, evident discrepancy of the chemical component and crystallization state will show up. The discrepancy will lead to the imperfection field at the medial plane such as the 1^{st} harmonic. In the numerical calculation of the magnetic field, it is assumed the material for 1/4 of the top/bottom yoke is Q235, and the other 3/4 1008#. The maximum amplitude of the 1^{st} harmonic at the medial plane is ∼4 Gauss. It is not as sensitive as that from the sectors.

4 RF cavity design

In order to increase the energy gain per turn, to reduce the beam loss and enhance the vertical focusing at the high energy region, it is required that the spread angle of the Dee be expanded as much as possible and the Dee voltage be increased along with the radius. In the 100 MeV compact cyclotron, the two cavities are located in two opposite valleys and their RF requirement is as follows[3]: the resonant frequency is approximately 43—45 MHz, the accelerating voltage at the central region is 60 kV, and about 120 kV at the large radius, the stability of frequency is better than 1×10^{-6}, the Dee voltage 5×10^{-4}, and the phase angle within 0.1°.

4.1 Cavity design with double stems

In the case when the cavity takes the structure of single stem as in many classical designs[4, 5], the resonant frequency could easily meet the requirement,

while the Dee voltage distribution fails to increase at the outer radius. To solve the problem, the double-stem structure is taken into consideration, and its structural outline is shown in Fig. 5. Through the adjustment of the location, the dimension of the inner stems and the coupling capacitor, the cavity frequency is 44.32 MHz, and the Q value is 10600. The Dee voltage distribution meets the requirement in different regions, as shown in Fig. 6.

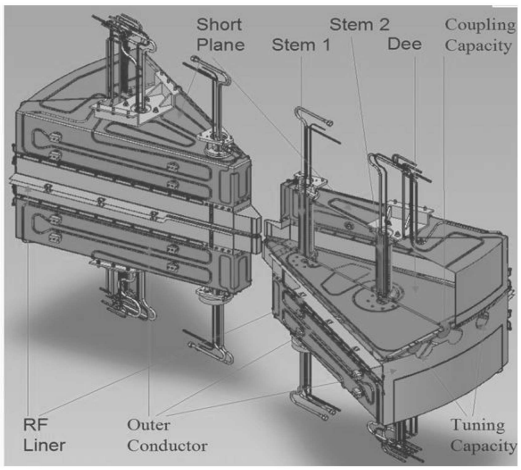

Fig. 5. The structure of double-stems cavity.

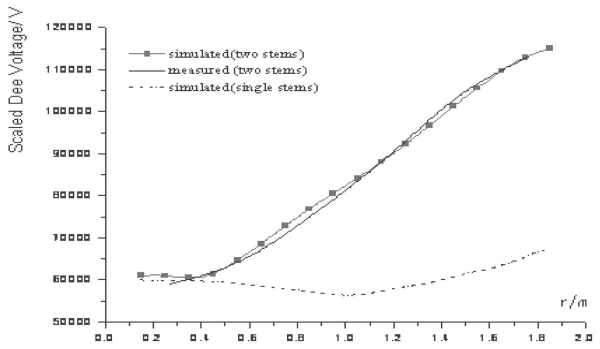

Fig. 6. Dee Voltage, simulation and measurement.

4.2 Model test

Based on the double-stem structure design for the cavity, a wooden experimental cavity covered by copper was built and measurements were conducted, including eigen resonant frequency of the cavity, Dee voltage distribution, matching, etc. The measurement result of cavity frequency is 44.27 MHz, and the voltage distribution curve from the central region to the extraction region is shown in Fig. 6. Fig. 6 shows that the measured value agrees well with the simulated result for the Dee voltage distribution from the central region to the extraction region. The result from the single stem structure is also given for comparison. The dissipated RF power on the cavity and thermal distribution are also investigated numerically and published else where[6].

5 Injection and central region design

The central region refers to the area where the beam travels for the first several turns. In this low energy region, the orbit traveling inside the Dee gap is relatively long, and the influence by the Dee gap shape and dimension as well as the RF phase turns out to be obvious. The study on the central region design mainly focuses on the orbit tracking in this region under the comprehensive affect of magnetic, HV electric and RF fields. Based on that, the optimized injection condition is obtained, by adjusting not only the injection energy, inflector and Dee gap, but also the tips of the poles, and consequently followed up by the magnetic field in the central region, e.g. adjusting the bump. That requires the beam centering and minimum oscillating amplitude in both radial and vertical directions. Moreover, the RF phase acceptance of 40° is crucial for this H^-, high intensity machine. Along with the simulation, Fig. 7 shows the orbit tracking results in the central region.

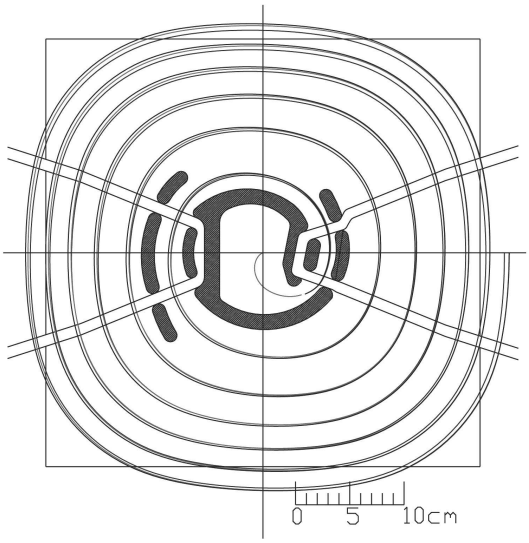

Fig. 7. The central orbits with different initial conditions.

The axial injection line[7] of CYCIAE-100 serves to inject the H^- beams generated by multi-cusp source to the cyclotron center, and ensures good transmission efficiency and beam quality. The extracted beam intensity for CYCIAE-100 is required to reach 200 μA, and it is planned to provide pulsed beam as well. In order to get a high average beam

intensity and to be capable of providing pulsed beam, two beam lines for the axial injection are considered in the design, corresponding to line 1 and line 2 respectively. Fig. 8 demonstrates the layout for the two injection lines. The two lines are perpendicular to each other, and share some part of the elements. Line 1 takes advantage of the neutralization of H^- beam to solve the constant intensified beam injection. To obtain a high neutralization rate, the transverse focusing applies all magnetic elements (SSQQQ). Line 2 is mainly designed to provide pulsed beams. Since the process of neutralization is hard to establish for pulsed beam injection, all elements used for chopping, bunching and transverse focusing are electrostatic. Fig. 9 shows the transverse profile during the injection for line 1 and line 2 respectively. The space charge effect, stray field from the main magnet, and the HV e-field of the inflector are taken into account during the optics matching.

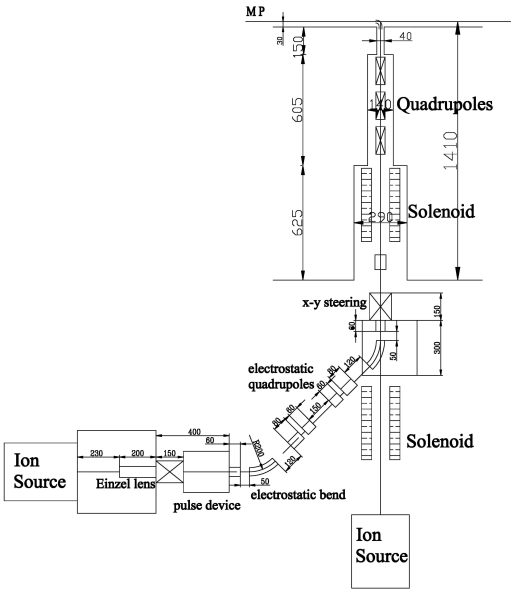

Fig. 8. The layout of axial injection lines in CYCIAE-100.

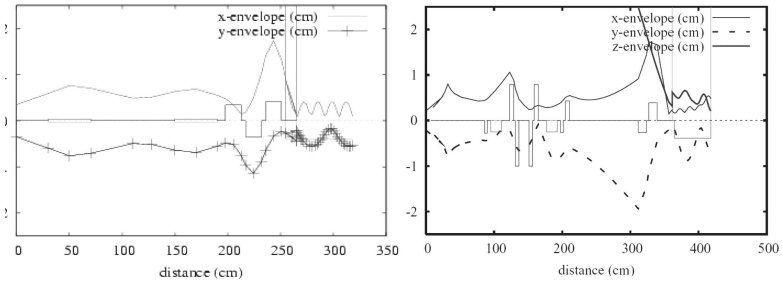

Fig. 9. The transverse profile of 1# and 2# injection line.

6 Design for extraction and beam lines

In CYCIAE-100, the extraction system[8] applies dual stripping, the extracted beam intensity is 200 μA, and its energy range is 75—100 MeV. The advantages of stripping extraction concern several aspects, including achieving synchronous multi-beam extraction, and continuously adjustable energy. The extraction efficiency is usually up to 99%. The stripping probe used for extraction is inserted into the machine from the hill gap, which could be accurately controlled in the radial direction and rotating of the foil orientation. The extracted beams of different energies will reach the center of combination magnet (at R=2.75 m, θ=100°) and are combined into a beam line. Fig. 10 shows the location of the stripping positions for different energies and the combination magnet.

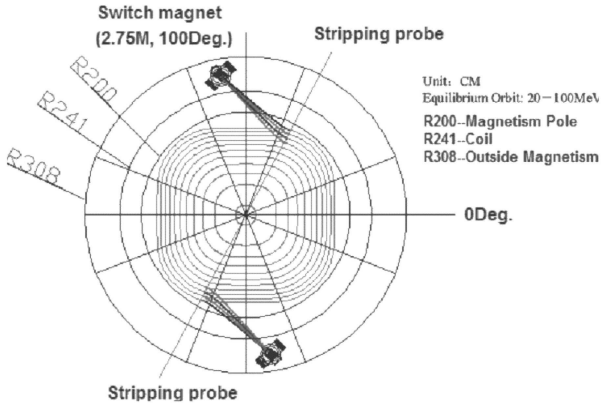

Fig. 10. The locations of probe and the combination magnet.

The location of the stripping probe is calculated with the code CYCTRS developed by CIAE, as well as a number of other codes from other institutes. The

result is shown in Table 3.

Table 3. Energy and corresponding extraction position.

energy/MeV	radius/M	$\theta/(^\circ)$
100	1.87553	59.626
90	1.7962	58.9586
80	1.70864	58.388
70	1.6120	57.806

For the optics matching to the 7 beam lines downstream, the matrix between stripping point and the center of combination magnet when the beam travels in the fringe field, is calculated by tracking the central orbit and the other 8 particles on the phase ellipses with CYCTRS, GOBLIN[9] and STRIP-UBC[10]. The initial ellipses on the stripping foil are calculated by multi-particle simulation of the acceleration with COMA[11]. The current result of the matrix at the extraction region is:

$$M_s = \begin{pmatrix} 0.992 & 0.206 & 0 & 0 & 0 & 0.656 \\ -0.431 & 0.918 & 0 & 0 & 0 & 4.080 \\ 0 & 0 & 0.503 & 0.192 & 0 & 0 \\ 0 & 0 & -2.619 & 0.988 & 0 & 0 \\ -0.433 & -0.024 & 0 & 0 & 1 & 1.607 \\ 0 & 0 & 0 & 0 & 0 & 1 \end{pmatrix}.$$

The extracted beams of energy from 70 to 100 MeV are tracked, transported into the center of combination magnet, as shown in Fig. 11. Fig. 12 demonstrates the dispersion effect at the extraction region. All the beam lines design is finished based on the results of optics investigation in the extraction region[12].

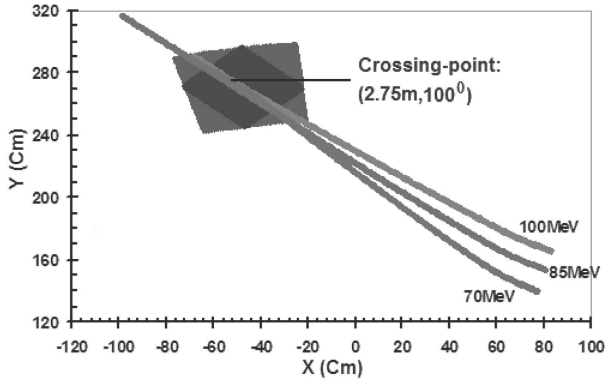

Fig. 11. Extracted trajectories for particles at different energy.

7 Conclusion

The physics design for CYCIAE-100 has been accomplished on the basis of the current industrial level in China well taken into account. So far the steel for main magnet is ready. The major parts, including the main magnet, cavities, RF amplifier, etc. are being constructed.

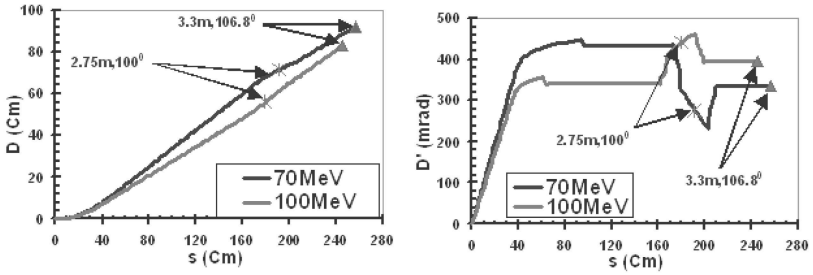

Fig. 12. Dispersion effects for the extracted energy of 70 MeV and 100 MeV.

References

1 ZHANG Tian-Jue et al. 17th ICC2004. Tokyo. 497—501
2 ZHANG Tian-Jue et al. NIM-B, 2007, **261**: 25–3
3 WANG Xiu-Long et al. 17th ICC2004. Tokyo. 330—332
4 FAN Ming-Wu et al. Chinese Science Bulletin, 1995, **40**(20): 1825 (in Chinese)
5 Eiche M et al. 13th ICC1992. Canada. 515—518
6 WEI Su-Min et al. 18th ICC2007, Italy. 461—463
7 YAO Hong-Juan et al. Rev. of Sci. Instrum., 2008, **79**(2): 02C708-02C708-3
8 AN S Z et al. 18th ICC 2007, Italy. 69—71
9 GOBLIN User Guide and Reference, TRI-CD-90-01, TRIUMF
10 Baartman R, Rao Y N. TRI-DN-05-4, TRIUMF
11 Kost C J, Mackenzie G H. IEEE Transactions on Nuclear Science, 1975, **NS-22**(3) June
12 WEI Su-Min et al. NIM-B, 2008, **266**: 4697—4701